Utilization of Hollow Silica Nanospheres for Thermal Insulation Purposes

Sohrab Alex Mofid[a*], Bjørn Petter Jelle[ab] and Tao Gao[a]

[a]Norwegian University of Science and Technology (NTNU),
Department of Civil and Transport Engineering, NO-7491 Trondheim, Norway.
[b]SINTEF Building and Infrastructure,
Department of Materials and Structures, NO-7465 Trondheim, Norway.
[*]Corresponding author: sohrab.mofid@ntnu.no (e-mail), +47-93051989 (phone).

ABSTRACT

A great deal of attention has been paid to thermal insulation as it plays a significant role in improving the energy efficiency within the building and construction sector. There is an ever-increasing demand for advanced thermal insulation materials that show superior performance to that of the conventional ones. The state-of-the-art thermal insulation materials and solutions, such as vacuum insulation panels (VIP) and silica aerogels, and the emerging ones like nano insulation materials (NIM), are under rapid development and show a promising potential. Hollow silica nanospheres (HSNS) may be a promising candidate for achieving high performance super insulation materials (SIM). This study investigates synthesis parameters and properties of HSNS with the aim of reaching low thermal conductivity by exploiting the Knudsen effect. The experiments are carried out to optimize thermal performance based on variation of structural parameters like e.g. HSNS shell thickness and inner diameter.

Keywords: hollow silica nanosphere, HSNS, nano insulation material, NIM, thermal insulation.

1 INTRODUCTION

The last decades have witnessed a rapid growth of research and development activities applying nanotechnology in various fields including the construction industry that seek out a way to advance building materials/components by using a variety of nanomaterials [1-3]. It has been shown that the application of nanotechnology can significantly enhance important characteristics of building materials, such as durability and strength, and in addition enrich them with new useful properties [3-5], allowing the adaption of known theoretical principles in practice. Present-day worldwide effort is to limit the energy usage in the building sector by minimization of the heat loss and exacerbation of the requirements for thermal insulation. Enhancement of insulation properties within the building sector is a challenging task to fulfil and is associated with making compromises in both financial, functional and architectural areas. Therefore, new, innovative and more effective materials are currently being sought. Among them are insulation materials with super-low thermal conductivity and smaller dimensions which may revolutionize the development of high performance thermal insulation materials.

Conventional thermal insulation materials, like mineral wool, expanded polystyrene (EPS), extruded polystyrene (XPS) and polyurethane (PUR) foam have high thermal conductivities around 30-40 mW/(mK) (PUR: 20-30 mW/(mK)). Their application have not been fully satisfactory for several reasons, e.g. architechtural restrictions, safety issues and material consumption and costs. Traditional thermal insulators are distinguished by how they trap a gaseous material, i.e. in a fibrous, cellular or granular material [6].

New and improved state-of-the-art thermal insulation materials or solutions such as vaccum insulation panels (VIP) and silica aerogels may be more favourable to use due to their lower thermal conductivity. VIPs have a centre-of-panel thermal conductivity of typical 4 mW/(mK) in the pristine non-aged condition, wheres silica aerogels have values between 12-20 mW/(mK). However, both VIP and silica aerogels as well present certain weaknesses like fragility, perforation vulnerability (VIP), loss of vacuum by air and moisture diffusion (VIP) and relatively high costs. Similarly to the distinction in conventional thermal insulators, current state-of-the-art thermal insulators are distinguished by how they fulfil rarefaction of the gas, i.e. by a nanoporous solid structure or by application of a partial vaccum, in contrast to the fact that the best results may be obtained with the combination of both [6].

Hence, nanoengineering has been employed to study and demonstrate nano insulation materials (NIM) based on hollow silica nanospheres (HSNS) which have size-dependent thermal conduction and may be readily controlled over a large range [7]. Silica represents one of the best candidates for achieving HSNS as silica is the most abundant material in nature. This work gives an overview of the HSNS synthesis and characterizations and aim to reduce the thermal conductivity by modification of structural parameters such as the shell thickness of the hollow nanospheres.

2 EXPERIMENTAL

2.1 General

The materials used during the synthesis are summarized in Table 1 below.

Table 1: Materials used during the synthesis of HSNS (further details in the following section).

Raw materials	Volume (mL)	Mass (g)	Material supplier
Step 1: Synthesis of polystyrene nanospheres			
H_2O	110	110	In-place
Styrene	-	10	Sigma Aldrich
PVP	-	1.5	Sigma Aldrich
KPS	-	0.1	Sigma Aldrich
Step 2: Coating polystyrene nanospheres with silica			
Ethanol	332[a]	182	Sigma Aldrich
PS[b]	-	12	In-place
NH_4OH	12	-	Sigma Aldrich
TEOS	15	-	Sigma Aldrich

[a] Including ethanol used for washing the particles.
[b] PS nanosphere suspension.

2.2 Monodisperse PS Nanospheres

Monodisperse polystyrene (PS) nanospheres were first prepared and used as templates for the growth of silica coatings. The resulting PS spheres are depicted in the transmission electron microscope (TEM) images in Fig.1.

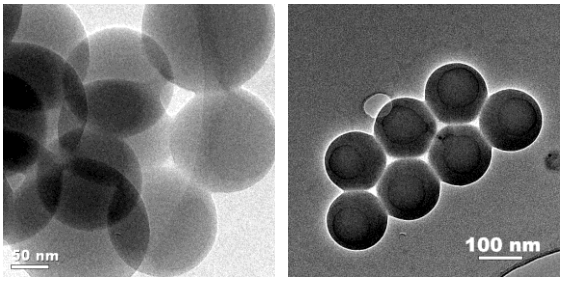

Figure 1: TEM images of monodisperse PS nanospheres with 150 nm diameter size.

For the particular synthesis, 1.5 g polyvinylpyrrolidone (PVP) was dissolved in 100 mL distilled water under ultrasonic irradiation, whereafter 10 g styrene solution was added to the mix. The obtained styrene/PVP solution was heated up to 70°C under constant stirring at 500 rpm. Afterwards, 10 mL potassium persulphate (KPS) solution (0.15 g KPS in 10 mL water) was added drop-wise into the PVP/styrene solution to initiate the polymerization reaction. The polymerization reaction was kept at around 70°C for 24 h. After the reaction took place, the obtained PS nanosphere suspension was cooled down to room temperature for further use.

2.3 Silica Nanospheres

For the particular synthesis, 6 g of as-prepared PS suspension and 4 mL NH_4OH solution were added into 120 mL ethanol under constant stirring at 500 rpm for two identical samples twice, Then, 10 mL tetraethyl orthosilicate (TEOS) ethanol solution (50 vol% TEOS in ethanol) was added drop-wise. For one of the two sample solutions, the suspension was divided into two equal portions and another 10 mL TEOS ethanol solution (50 vol% TEOS in ethanol) was added drop-wise to one of the solutions in order to grow thicker shell structures with silica, whereas the second equal solution remained unchanged. The reaction system was stirred for 10–24 h to prepare core-shell type PS@SiO_2 nanospheres. After the reaction, the solid product was separated from the mother solution by centrifugation. The obtained sediment was washed with ethanol once again and finally kept drying at room temperature. Hollow silica nanospheres were readily obtained by annealing the PS@SiO_2 nanospheres at 500°C in air for 5 h, with resulting HSNS as shown in the TEM images in Fig.2.

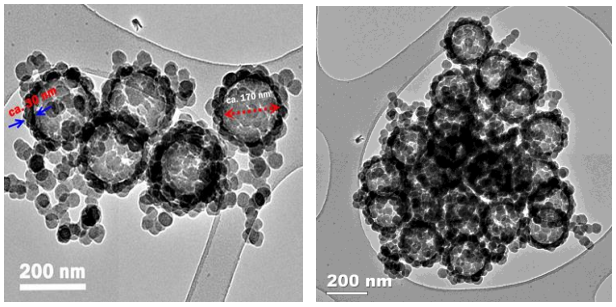

Figure 2: TEM images of HSNS with mean diameter of 150 nm and shell thickness of around 30 nm.

2.4 Characterization

Transmission electron microscope (TEM, JEM-2010) and scanning electron microscope (SEM, Hitachi S-5500) were employed to characterize the morphology and nanostructure of the as-synthesized items. Thermal conductivity of the obtained bulk materials was analyzed by using a Hot Disk Thermal Constants Analyzer (TPS 2500S). A disk-type Kapton Sensor 5465 with radius 3.189 mm was used. The sensor, which acts as heat source and temperature recorder, was sandwiched between two parts of powder samples. Temperature increase of the samples as a function of time was recorded to compute the thermal conductivity (uncertainty ~ 5%). The final thermal conductivity value reported was the arithmetic mean of four

individual measurements under different conditions (heating power 0.02–0.2 W; measurement time 1–320 s).

3 THERMAL PROPERTIES OF HSNS

The thermal conductivity of the HSNS can be understood by the size-dependent thermal conduction at nanometer scale [8,9]. Hence, the low thermal conductivity of the HSNS contributions from various thermal conduction mechanisms such as gaseous, solid, radiation and convection heat transport can determine the measured thermal conductivity of the HSNS.

3.1 Gaseous Thermal Conductivity

Gaseous thermal transport in a space with small dimensions can be explained by the Knudsen effect, where the mean free path of the gas molecules is larger than the pore diameter of the material. The gaseous thermal conductivity, including the gas and pore wall interaction, may according to the Knudsen effect be written as [10]:

$$\lambda_g = \frac{\lambda_{gas,0}}{1+2\beta Kn} \tag{1}$$

where

$$Kn = \frac{l_{mean}}{\delta} = \frac{k_B T}{\sqrt{2}\pi d^2 p\delta} \tag{2}$$

where λ_g is the gaseous thermal conductivity in the pores (W/(mK)), $\lambda_{g,0}$ is the gas thermal conductivity in the pores at standard temperature and pressure (STP), Kn is the Knudsen number indicating the ratio between the mean free path l_{mean} of gas molecules (m) (for air, $l_{mean} \approx 68$ nm at ambient condition) and δ the characteristic pore diameter (m), k_B is the Boltzmann's constant ($1.38 \cdot 10^{-23}$ J/K), T is the temperature (K), d is the gas molecule collision diameter (m), p is the gas pressure in the pores (Pa), β is a coefficient (between 1.5 and 2.0) characterizing the energy transfer (in)efficiency in terms of collision of gas molecules with the solid structure [7]. A lower pressure gives a longer mean free path which in turns gives a larger Knudsen number, i.e. a lower gaseous thermal conductivity. According to Eq.2, it is obvious that for pores with diameters of a few nanometers, the Knudsen effect becomes very large (small Knudsen number), thus resulting in reduced gaseous thermal conductivity. In this study, the synthesized HSNS have pore diameters of about 150 nm, which in turn can theoretically reduce the gaseous thermal conductivity down to10 mW/(mK).

3.2 Solid Thermal Conductivity

To further understand the measured thermal conductivity of HSNS due to variation in shell thickness, the solid-state conduction has to be taken into account. Theory of size-dependent thermal conductivity at nanoscale level for semiconductor systems is explained by Liang and Li [11]. Accordingly, the solid-state thermal conductivity of solid nanospheres λ_N can be given as:

$$\frac{\lambda_N}{\lambda_B} = p \cdot \exp\left(-\frac{l_0}{D}\right) \cdot \left[\exp\left(\frac{1-\alpha}{D/D_0 - 1}\right)\right]^{3/2} \tag{3}$$

where λ_B is the thermal conductivity of the bulk material, l_0 is the phonon mean free path at room temperature, D is the featured size (e.g. diameter of nanoparticles), D_0 and α are material constants, p is a factor reflecting the surface roughness, $0 \le p \le 1$, where $p \to 1$ represents a smoother surface which results in higher probability of specular phonon scattering, whereas $p \to 0$ corresponds to a rougher surface with higher probability of diffusive phonon scattering [12-13]. Related to our HSNS, given the same inner diameter, one may conclude that a thinner HSNS shell thickness, and thus smaller D in Eq.3, may result in lower solid-state thermal conductivity than a thicker shell thickness. In general, a more tortuous thermal conduction path leads to a lower solid-state thermal transport and conductivity. Although material-dependent parameters make it difficult to calculate an exact thermal conductivity value, as the contact area between adjacent spheres are typically within a few nanometers from each other [14], in general the contribution from the solid-state thermal conductivity in such materials is very small [15].

4 RESULTS AND DISCUSSION

This work gives an overview of the pathway of achieving NIM by based on HSNS. In general, the advantage of nanoporous materials' size-dependent thermal conduction at nanometer scale is the main reason for conducting such studies [16-17]. Thermal properties of HSNS may well depend on several structural parameters, such as the shell thickness of the hollow spheres, inner diameter, chemical composition of the shell materials and density of the hollow spheres [18]. Consequently, by modification of these structural parameters, the thermal performance of hollow spheres may be optimized and controlled over a large range.

HSNS can be prepared through different methods, of which the template-assisted approach represents presumably the most straightforward method with numerous advantages [19]. PS was chosen as the template material for the growth of HSNS because of the fact that PS nanospheres can be prepared with controlled diameters through varying the PVP/styrene weight ratio and surface properties [20-24]; furthermore, can be easily removed either by heating or dissolution [22-24]. In this study, PS nanospheres of 150 nm was prepared with a PVP/styrene ratio of 0.15. The small size and large surface-to-volume ratio, and that the PS nanosphere surfaces are very active, make PS nanospheres ideal nucleation sites for growth of silica. Considering the small size of PS nanospheres one could expect according to the Knudsen effect (Eq.1 and 2)

that the gaseous thermal conductivity may further be suppressed by reducing the inner pore diameter controlled by the PVP/styrene ratio.

The HSNS shells consist of silica nanoparticles produced from hydrolysis of TEOS that is captured and deposited on the surface of the PS nanospheres. The silica nano particle size may also depend on several experimental parameters such as NH_4OH and TEOS concentrations and reaction temperature [25].

Variation of thermal conductivity with respect to shell thickness is given in Table 2.

Table 2: Average thermal conductivity λ_{avg} for HSNS samples of different shell thicknesses L and constant inner diameter D.

Sample	λ_{avg} (mW/(mK))*	L (nm)	D (nm)
A	36 ± 1	10 ± 2	155 ± 5
B	45 ± 2	20 ± 3	162 ± 7
C	59 ± 3	30 ± 4	166 ± 9

*The uncertainty is calculated as two times the standard deviation of the mean, i.e. within a confidence interval of 95.45%.

It should be mentioned that variation of thermal conductivity values was obtained within one set of testing procedure, where values obtained from combinations of heating power and measurement time with Hot Disk apparatus were analysed, and hence finally an average of the conductivity values were calculated, each of them based on three samples.

5 CONCLUSIONS

Hollow silica nanospheres (HSNS) exhibit great flexibilities of modifying their properties by tuning the corresponding structural features. The structural features can be controlled by using the polystyrene (PS) nanosphere templates with different properties and/or use of different precursors like e.g., TEOS or Water glass as a structure for shell thickness growth. HSNS with inner pore diameters of ~ 150 nm and varying shell thicknesses of 10, 20 and 30 nm have been prepared. It was found that the thermal conductivity decreased with decreasing HSNS shell thickness which is in agreement with the theoritical background. Though experimentally challenging, future studies may be conducted in order to make PS nanospheres with reduced inner diameters, e.g. down to 30-50 nm, in an attempt to further lower the thermal conductivity according to the Knudsen equation. Due to the nature of HSNS and their properties for thermal insulation applications, further studies and development are worth pursuing.

ACKNOWLEDGEMENTS

We thank Yingda Yu (NTNU) for his contribution with the characterization by transmission electron microscopy.

REFERENCES

[1] Zhu, W.; Bartos, P. J. M.; Porro, A. *Mater. Struct.*, **37**, 649–658, 2004.
[2] Lee, J.; Mahendra, S.; Alvarez, P. J. J. *ACS Nano*, **4,** 3580–3590, 2010.
[3] Raki, L.; Beaudoin, J.; Alizadeh, R.; Makar, J.; Sato, T. *Materials*, **3**, 918–942, 2010.
[4] Lee, J.; Mahendra, S.; Alvarez, P. J. J. *ACS Nano* , **4**, 3580–3590, 2010.
[5] Raki, L.; Beaudoin, J.; Alizadeh, R.; Makar, J.; Sato, T. *Materials*, **3**, 918–942, 2010.
[6] F.Pacheco-Torgal, M.V. Diamanti, A.Nazari, C-G Granqvist, "Nanotechnology in eco-efficient construction", 188-189, 2013.
[7] Jelle, B. P.; Gao, T.; Sandberg, L. I. C.; Tilset, B. G; Grandcolas, M.; Gustavsen, A. *International Journal of Structural Analysis and Design*, **1**, 43-50, 2014.
[8] Cahill, D. G.; Ford, W. K.; Goodson, K. E.; Mahan, G. D.; Majumdar, A.; Maris, H. J.; Merlin, R.; Philipot, S. R. *J. Appl. Phys.*, ***93***, 793–818, 2003.
[9] Heino, P.; Ristolainen, E. *Phys. Scripta* **,** *T114*, 171–174, 2004.
[10] Jelle, B. P. *Energy and Buildings*, **43**, 2549-2563, 2011.
[11] Liang, L.; Li, B. *Phys. Rev. B*, **73**, 153303, 2006.
[12] Liu, L.; Chen, X. *J. Appl. Phys.*, **107**, 033501, 2010.
[13] Teja, A. S.; Beck, M. P.; Yuan, Y.; Warrier, P. *J. Appl. Phys*., **107**, 114319, 2010.
[14] Desai, T. G. *Appl. Phys. Lett*., **98**, 193107, 2011.
[15] Liao, Y.; Wu, X.; Liu, H.; Chen, Y. *Thermochim. Acta*, **526**, 178–184, 2011.
[16] Cahill, D. G.; Ford, W. K.; Goodson, K. E.; Mahan, G. D.; Majumdar, A.; Maris, H. J.; Merlin, R.; Philipot, S. R. *J. Appl. Phys*., **93**, 793–818, 2003.
[17] Heino, P.; Ristolainen, E. *Phys. Scripta*, T**114**, 171–174, 2004.
[18] Gao, T.; Sandberg, L. I. C.; Jelle, B. P.; Gustavsen, A. In "Fuelling the Future: Advances in Science and Technologies for Energy Generation, Transmission and Storage", Mendez-Vilas, A. A. (Ed.); *BrownWalker Press: Boca Raton*, 535–539, 2012.
[19] Guerrero-Martínez, A.; Pérez-Juste, J.; Liz-Marzán, L. M. *Adv. Mater*., **22**, 1182–1195, 2010.
[20] Yang, J.; Lind, J. U.; Trogler, W. C. *Chem. Mater*., **20**, 2875–2877, 2008.
[21] Du, X.; He, J. *J. Appl. Polym. Sci*., **108**, 1755–1760, 2008.
[22] Zou, H.; Wu, S.; Ran, Q.; Shen, J. *J. Phys. Chem. C*., **112**, 11623–11629, 2008.
[23] Chen, M.; Wu, L. M.; Zhou, S. X.; You, B. *Adv. Mater*., **18**, 801–806, 2006.
[24] Cao, S. S.; Jin, X.; Yuan, X. H.; Wu, W. W.; Hu, J.; Sheng, W.C. *J. Polym. Sci. Part A: Polym. Chem*., **48**, 1332–1338, 2010.
[25] Stöber, W.; Fink, A.; Bohn, E. *J. Colloid Interf. Sci*., **26**, 62-69, 1968.